RESEARCH PAPER

Critical Analysis of Spectral Characteristics of FBG Sensor for Precise Monitoring in Medical Sensing Applications

Santosh Jotiram Jagatap[1,2], Dr. Ashok Jetawat [3], Dr. Saurabh Mehta[4], Dr. Jayshree Jetawat[5]

[1,3,5] Department of Computer Engineering, Pacific Academy of Higher Education and Research, Udaipur, Rajasthan
[2] Vidyalankar Institute of Technology, Mumbai.
[4]Department of Electronics and Telecommunication Engineering, Vidyalankar Institute of Technology, Mumbai.
Email: santosh.jagtap0106@gmail.com, santosh.jagtap@vit.edu.in, drashokjain61@gmail.com, saurabh.mehta@vit.edu.in, drjayshreejain@gmail.com

ABSTRACT:
Fiber Bragg Grating sensors are most promising to fulfill needs of transformed healthcare standards. Optical fiber sensors use optical detection principle rather than electronic principle used in conventional electronic sensors. This not only offers advantage of small size and light weight but also offers high measurement sensitivity in noisy environment. FBGs offers high sensitivity compared to conventional electronic sensors as optical signal is isolated from noise and electromagnetic interference. The study of the structural parameters and spectral properties of fiber Bragg grating is equally important in medical sensing applications. The structural design of fiber Bragg grating sensor consist of grating which is formed by introducing periodic variation of refractive index of core. Grating reflects specific wavelength known as Bragg wavelength. The external stimulus such as temperature, strain and pressure introduces shift in the reflected Bragg wavelength. The strength of reflected Bragg wavelength known as reflectivity depends on its structural parameters such as grating length, period and modulation index. The spectral response of fiber Bragg grating sensors shows some undesired reflected wavelengths along with desired Bragg wavelength. These undesired wavelengths are known as side lobe levels and contributes noise affecting detection sensitivity. Hence high reflectivity and low side lobe levels are essential for high sensitivity and precise measurement of medical parameters. In this research work, the effect of structural parameters on spectral response is demonstrated by developing mathematical and simulation model. The sensor design is optimised for high reflectivity and minimum side lobe levels. The apodization techniques are introduced and comparative analysis is done to get desired level of reflectivity and side lobe levels. The proposed fiber Bragg grating sensor model is suitable for precise monitoring of healthcare parameters in medical sensing applications.

Keywords: Healthcare parameters, Fiber Bragg grating Sensor, Spectral response, Reflectivity, Side lobe levels, Apodization techniques.

How to cite this article: Jagatap SJ, Jetawat A, Mehta S, Jetawat J. Critical Analysis of Spectral Characteristics of FBG Sensor for Precise Monitoring in Medical Sensing Applications. Int J Drug Deliv Technol. 2026;16(17s): 1-7. DOI: 10.25258/ijddt.16.17s.1

1.INTRODUCTION

The modern healthcare system has created increased demand for sensors capable of providing high sensitivity, high precision, accurate and reliable measurements of healthcare parameters. Measurement of vital signs such as body temperature, heart rate, respiration rate and blood pressure requires sensors which can detect extremely small variations in electrically noisy environment. Vital signs provide essential information of body's physiological function hence in clinical setting their accurate measurement and assessment is critical. Traditional methods for measuring vital signs, such as sphygmomanometers for blood pressure, electrocardiograms for heart rate, and spirometers for respiration rate, involve cuff inflation, electrode placement, and forced breathing manoeuvres. These methods can be uncomfortable, invasive, and do not allow for continuous monitoring during daily activities, as they are still associated with some degree of discomfort to the patient and [1]. Also, these traditional electronic sensors are susceptible to noise and electromagnetic interference. The extensive literature review on biosensors shows limitations in their practical implementation [2]. These limitations motivate researchers and healthcare professionals to find alternative sensing technology that can provide higher accuracy and precise measurement of healthcare parameters. The fiber Bragg grating (FBG) is emerging technology for biomedical applications due to their small size, biocompatibility, multiplexing capability and immunity to EMI [3]. The operating principle of FBG is based on wavelength shift which responds to physiological parameters such as temperature, strain and pressure. The optical detection principle makes them more suitable for measurement of physiological parameters in electromagnetic environments where conventional sensors fail to maintain accuracy. Additionally, FBGs compactness allows them to integrate with modern wearable systems for continuous and remote monitoring of healthcare parameters [1].

The spectral characteristics of the FBG are equally important in medical sensing applications. The in-depth study of spectral characteristics such as reflectivity and side lobe levels allows researchers and medical practitioners to determine their impact on sensitivity and accuracy in measurement. The reflectivity refers to strength of desired reflected Bragg wavelength due to input measurand. The unwanted reflected wavelengths with desired Bragg wavelength are known as side lobe level (SLL). Figure 1 shows the spectral response of the FBG in which main lobe represents strength of desired signal, i.e. reflectivity while adjacent to main lobe it

shows undesired SLLs. The undesired side lobe levels contribute to the noise and affect the detection sensitivity. Hence in medical sensing application high reflectivity and low side lobe levels are desirable for accurate and precise measurement of healthcare parameters. The reflectivity and SLLs are primarily dependent on the structural parameters of FBG sensors. The structural parameters such as grating length, grating period and modulation index allow designers to control the reflectivity and SLLs.

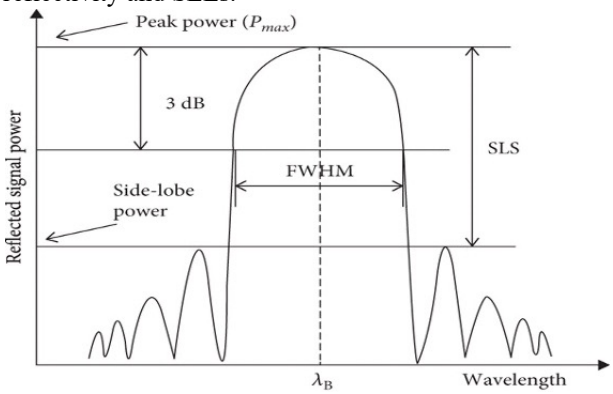

Figure 1: Spectral characteristics of FBG Sensor [4]

The focus of this research work is to demonstrate the effect of structural parameters on reflectivity and SLL. The critical analysis is performed to show the effect of grating length, period and modulation index on reflectivity and SLL. The outcome of the analysis is used to optimize FBG sensor design to obtain high reflectivity and low SLLs. The apodization technique is used to investigate the performance of uniform and Gaussian profile FBG sensor. This work provides guidelines for researchers and medical professionals to design and select appropriate sensing solutions for precise measurement of healthcare parameters.

2. FBG Sensors Theory

Fiber Bragg Grating (FBG) technology is one of the most popular choices for optical fiber sensors for strain or temperature measurements due to their high sensitivity [5]. The periodic variation in refractive index (R.I.) is introduced in the core of the optical fiber is known as Grating. The length over which this variation is introduced is known as Grating length. The period of the R.I. variation is known as grating period and strength of R.I. variation is known as modulation index. Figure 2 represents typical structure of the FBG sensor. The light source launches the input signal to FBG sensor. Grating reflects the specific wavelength which satisfies the Bragg condition. This reflected wavelength is known as Bragg wavelength and is given by equation (1).

$$\lambda_B = 2n_{eff}\Lambda \quad (1)$$

where n_{eff} is known as effective refractive index and Λ is the grating period.

The external stimulus such as temperature and strain and pressure introduce shift in the Bragg wavelength. The strain (ε) and temperature (T) affect this wavelength and shifts it from its value defined by equation (1).

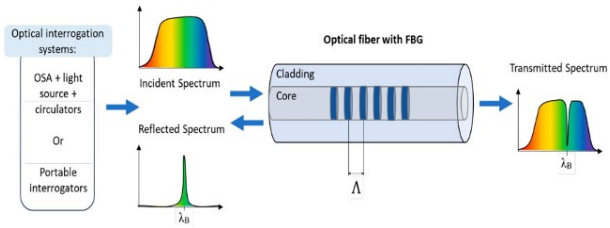

Figure 2: FBG Sensor Structure [1]

The wavelength shift due to strain and temperature is given as,

$$\frac{\nabla\lambda_B}{\lambda_B} = K_\varepsilon\varepsilon + K_T T \quad (2)$$

Where K_ε *and* K_T are known as strain and temperature sensitivities respectively.

The first term of equation (2) represents effect of strain, and second term represents effect of temperature. The change is strain and temperature changes grating period and effective modulation index. This gives shift in the Bragg wavelength. The measurement of wavelength shift allows to measure physiological parameters such as body temperature, heart rate, respiration rate and blood pressure.

3. Mathematical Model of FBG Sensor

FBG sensor modelling and simulation serve as fundamental tools for designing, optimizing, and validating sensor performance across a wide range of applications. They not only help in understanding the underlying physics of FBG operation but also facilitate cost-effective development by reducing reliance on extensive experimental setups. Mathematical models, typically derived from coupled-mode theory (CMT) and transfer matrix methods (TMM), are used to describe forward and backward propagating electromagnetic field in layered medium [6]. This allows to obtain transmission and reflection spectra regardless of complexity of grating [7]. key performance parameters such as reflectivity, transmission spectrum, bandwidth, SLL and sensitivity are determined from spectral response.

3.1 Coupled Mode Analysis

Many models have been developed to describe the behaviour of Bragg gratings in optical fibers. The most widely used technique has been coupled mode theory, where the counter-propagating fields inside the grating structure, obtained by convenient perturbation of the fields in the unperturbed waveguide, are related by coupled differential equations. The basic idea of the CMT method is that the modes of the unperturbed or uncoupled structures are defined and solved first. Then, a linear combination of these modes is used as a trial solution to Maxwell's equations for complicated perturbed or coupled structures. After that, the derived coupled mode equations can be solved analytically or by numerical methods.

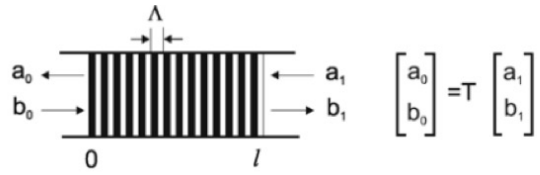

Figure 3: TMM Model of Uniform Bragg grating [8]

The electric fields of the backwardand forward-propagating waves can be expressed as,

$$E_a(x,t) = A(x).\exp[i(\omega t - \beta x) \quad (3)$$

$$E_b(x,t) = B(x).\exp[i(\omega t + \beta x) \quad (4)$$

where β is the wave propagation constant. The complex amplitudes $A(x)$ and $B(x)$ of these electric fields obey the coupled-mode equations.

$$= ikB(x)\exp[-i2(\Delta\beta)x] \quad (6)$$

$$= -ik^{*}A(x)\exp[i2(\Delta\beta)x]$$

where, A(x): Forward-propagating field amplitude, B(x): Backward-propagating field amplitude, x: Distance along the grating, $\Delta\beta = \beta - \beta_0$ is differential propagation constant, β is the propagation constant given by $\frac{2\pi n_0}{\lambda}$, $\beta_0 = \frac{\pi}{\Lambda}$, k is the coupling coefficient and k^* is the complex conjugate.

For uniform gratings, k is constant and it is related to the index modulation depth. For a sinusoidally-modulated refractive index the coupling coefficient is real, and it is given by,

$$k = \frac{\pi\Delta n_{mod}}{\Lambda} \quad (7)$$

Assuming that there are both, forward and backward inputs to the Bragg grating, and boundary conditions $B(0) = B0$ and $A(l) = A_1$, Following these assumptions, the closed-form solutions for x-dependencies of the two waves are,

$$a(x) = A(x)\exp(-i\beta_x) \quad (8)$$

$$b(x) = B(x)\exp(i\beta_x) \quad (9)$$

Therefore, the backward output (reflected wave), a_0, and the forward output (transmitted wave), b_1, from the grating can be expressed by means of the scattering matrix.

$$\begin{bmatrix} a_0 \\ b_1 \end{bmatrix} = \begin{bmatrix} S_{11} & S_{12} \\ S_{21} & S_{22} \end{bmatrix} \cdot \begin{bmatrix} a_1 \\ b_0 \end{bmatrix} \quad (10)$$

with $a_1 = A_1\exp(i\beta l)$. and $b_0 = B_0$, and

$$S_{11} = S_{22} = \frac{is\exp(-i\beta_0 l)}{-\Delta\beta\sinh(sl) + is\cosh(sl)} \quad (11)$$

$$S_{12} = S_{21} = exp(2i\beta_0 l)\frac{k\sinh(sl)}{-\Delta\beta\sinh(sl) + is\cosh(sl)} \quad (12)$$

Where $s = \sqrt{\kappa^2 - \Delta\beta^2}$ represents net propagation constant governing energy exchange between the two waves inside the grating. It determines how the reflected wave builds up along the grating length.

3.2 T Matrix Formulation

The Transfer Matrix (T-matrix) is a crucial tool in modelling FBGs, as it provides a systematic approach to analyse how light propagates through the grating. It relates the forward and backward propagating optical fields at the input and output of the FBG, allowing for the efficient calculation of key performance parameters like reflectivity and transmissivity. This method is particularly valuable because it simplifies complex calculations and accommodates both uniform and non-uniform grating profiles, including Gaussian and chirped structures. By dividing the FBG into small segments and calculating the T-matrix for each, the overall optical response can be accurately determined through matrix multiplication. This segmentation approach enables precise modelling of variations in the refractive index modulation along the grating, which is essential for optimizing parameters like SLL, bandwidth, and sensitivity. The T-matrix method is computationally efficient compared to directly solving coupled-mode equations, making it ideal for simulations and design optimizations. Ultimately, understanding and utilizing the T-matrix is fundamental for developing high-performance FBG-based systems used in applications such as biomedical sensing, structural health monitoring, and optical communication.

The T-matrix relates the input and output of the Bragg grating. Based on the scattering-matrix expression in (10), the T-matrix for the Bragg grating is,

$$\begin{bmatrix} a_0 \\ b_0 \end{bmatrix} = \begin{bmatrix} T_{11} & T_{12} \\ T_{21} & T_{22} \end{bmatrix} \cdot \begin{bmatrix} a_1 \\ b_1 \end{bmatrix} \quad (13)$$

$$T_{11} = T_{22}^{*} = exp(-i\beta_0 l)\frac{\Delta\beta\sinh(sl) + is\cosh(sl))}{is} \quad (14)$$

$$T_{12} = T_{21}^{*} = exp(-i\beta_0 l)\frac{k\,sinh(sl)}{is} \quad (15)$$

The refection coefficient of FBG sensor is calculated from the T Matrix. The reflectivity is defined as, ratio of reflected power to the input power,

$$R = \left|\frac{T_{21}}{T_{11}}\right|^2 \quad (16)$$

Hence,

$$R = \frac{sinh^2(sl)}{cosh^2 sl - \left(\frac{\Delta\beta}{\sqrt{s}}\right)^2} \quad (17)$$

Using, s =$\sqrt{\kappa^2 - \Delta\beta^2}$ in above equation, the reflectivity is determined by,

$$R(\lambda) = \frac{\boldsymbol{sinh^2\sqrt{\kappa^2-\Delta\beta^2}l}}{\left[\boldsymbol{cosh^2\left(\sqrt{\kappa^2-\Delta\beta^2}l\right)} - \left(\frac{\Delta\beta}{\sqrt{\sqrt{\kappa^2-\Delta\beta^2}}}\right)^2\right]} \quad (18)$$

This gives the equation to determine the reflectivity of the FBG sensor as a function of wavelengths.

The reflectivity of the FBG is function of the wavelength. The spectral dependence of the reflectivity is determined from eq. (18). The peak or maximum reflected power is obtained at the centre wavelength λ_B. At the Bragg wavelength $\lambda = \lambda_B$, $\Delta\beta = 0$. This is substituted in equation (18) which gives,

$$R = tanh^2(\kappa l) \quad (19)$$

This represents peak reflectivity of FBG sensor which gives maximum reflectivity at the Bragg wavelength.

4. Performance Enhancement by using Apodization Technique

The apodization function moderately modifies the refractive index modulation all over the length of the grating. The apodization is technique useful to supress side lobe levels. The apodization function is crucial for enhancing the proficiency of FBG sensor by terminating the side lobes in the reflectivity spectrum [9] [10]. There are several apodization functions and each of the profile function has a different impact on several applications [11] [12]. The index of the refractive profile for a uniform Bragg grating formed within the core of an optical fiber with an average refractive index n_0 , can be expressed as [13],

$$n(x) = n_0 + \Delta n \cos\left(\frac{2\pi x}{\Lambda}\right) \quad (20)$$

Where Δn is the amplitude of the induced refractive index perturbation, ʌ is the nominal grating period and x is the distance along the fiber longitudinal axis.

Apodized gratings have variations along the fiber in the refractive index modulation envelope (Δnαc) with constant grating period and constant DC refractive index function. The index of the refractive profile of Apodized can be expressed as,

$$n(x) = n_{co} + \Delta n_0 A(x).n_d(x) \quad (21)$$

Where n_{co} is the core refractive index, Δn_0 is the maximum index variation, $n_d(x)$ is the index variation function and A(x) is the Apodization function. The apodization function for different profiles is mathematically given as follows,

(i) Uniform Profile

The apodization function A(x)=1 defines uniform profile [14]. Hence from equation (21), the index of the refractive profile of uniform Grating can be expressed as,

A(x) = 1, 0 ≤ x ≤ L (22)

$$n(x) = n_{co} + \Delta n_0 . n_d(x) \quad (23)$$

This gives the uniform variation of refractive index along Grating length.

(ii) Gaussian Profile

The gaussian distribution of refractive index along the grating length is given as [4],

$$A(x) = exp\left(-ln2\left(\frac{2\left(x-\frac{L}{2}\right)}{0.5\,L}\right)^2\right) \quad 0 \le x \le L \quad (24)$$

The refractive index profile is then determined by substituting equation (24) in equation (21). Hence for Gaussian profile,

$$n(x) = n_{co} + \Delta n_0 . exp\left(-ln2\left(\frac{2\left(x-\frac{L}{2}\right)}{0.5\,L}\right)^2\right) n_d(x) \quad (25)$$

(iii) **Tanh Profile**

The apodization function for hyperbolic tan profile describes variation of refractive index along grating length defined is defined as [4]

$$A(x) = tanh\left(4\frac{x}{L}\right) * tanh\left(4\frac{1-x}{L}\right) \quad 0 \le x \le L \quad (26)$$

Substituting equation (26) in equation (21) gives,

$$n(x) = n_{co} + \Delta n_0 . \left(tanh\left(4\frac{x}{L}\right) * tanh\left(4\frac{1-x}{L}\right)\right) n_d(x) \quad (27)$$

In a gaussian profile, refractive index modulation gradually decreases from the centre of the grating towards the edges. Because the modulation decreases at the edges, the overall coupling efficiency is lower, leading to reduced reflectivity. However, the gaussian profile allows for a smoother reflection spectrum and better control of the reflection bandwidth. Hyperbolic tangent (tanh) profile refers to a non-uniform refractive index modulation where the coupling coefficient or grating strength changes gradually along the length of the grating, following a hyperbolic tangent function. Unlike uniform or Gaussian profiles, the tanh profile smoothly transitions between high and low index modulation, typically tapering the strength at both ends of the grating.

The desired level of reflectivity and SLLs can be obtained by selecting the suitable profile obtained from above analytical model. Apodization can help to improve performance at the cost of fabrication complexity.

5. Simulation Methodology

Several simulation and design tools can be employed for designing FBG sensors, each offering specific features tailored to FBG sensor development. In this work, OPTIGRATING tool is used to investigate the spectral characteristics of FBG sensor. Opti Grating is a powerful and user-friendly design software for modelling integrated and fiber optic devices that are assisted by optical gratings. Table gives typical FBG sensor specifications such as Strain optic coefficient, Photo elastic coefficient, Thermal expansion Coefficient and Thermo optic coefficient.

Table 1: Simulation Parameters for Characterizing FBG

Sr. No.	Simulation Parameters	Dimension
1	Grating Period	0.5338 µm
2	Modulation Index	0.0001
3	Core dimension	4.6 µm
4	Cladding dimension	62.5 µm
5	Wavelength	1550 nm
6	Strain optic coefficient	$0.2145\ \frac{1}{\mu\varepsilon}$
7	Photo elastic coefficient	0.121
8	Poisons Ration	0.17
9	Thermal expansion Coefficient	$5.5 \times 10^{-7}\ \frac{1}{c}$
10	Thermo optic coefficient	$8.6 \times 10^{-6}\ \frac{1}{c}$

The parameters given in table 1 define the physical and optical properties of the grating and directly influence key performance metrics such as reflectivity, bandwidth, and sidelobe level. The performance of FBG depends on certain design parameters which includes core- cladding dimensions, Grating period and length and modulation index. The effect of FBG structural parameters such as grating length and modulation index is shown on the spectral response. From the obtained response the optimum parameters are determined.

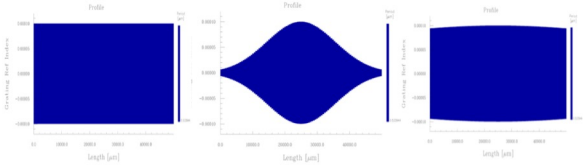

4(a). Uniform Profile 4(b). Gaussian Profile 4(c). Hyperbolic Tan profile

Figure 4: Apodization Profiles of FBG Sensor

Then the effect of apodization is observed with optimal selected parameters. The performance comparison of uniform, gaussian and hyperbolic Tan profile is investigated. The effect of grating length and modulation index is observed, and optimum length and modulation index are determined to get maximum reflectivity and SLL. Then the effect of uniform, gaussian and hyperbolic Tan profile is on the reflectivity and SLL are determined for optimized length and modulation index. Hence simulation methodology consists of first optimization of structural parameters to obtain optimum reflectivity and SLL. Then the apodization is performed for further improvement in performance of FBG sensor.

5. Simulation and Discussion on Results

The reflectivity and SLL vary with Grating Length, Grating period, Modulation index and Core Cladding dimensions. The effect of these parameters on FBG sensor performance in term of reflectivity and SLL is shown by simulating the uniform Bragg Grating with above specifications.

5.1 Effect of Grating length on Reflectivity and SLL.

The Grating length is varied from 10 mm to 30 mm and spectral characteristics are obtained. Figure 5 shows reflectivity spectrum of Uniform FBG at different lengths.

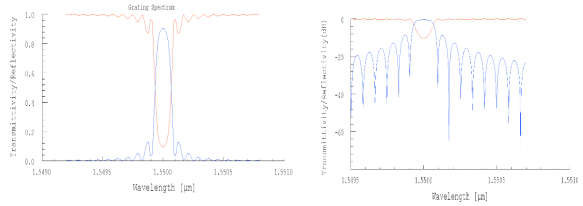

5(a) Reflectivity Spectrum at Grating Length of 10 mm 5(b) SLL Spectrum at Grating Length of 10 mm

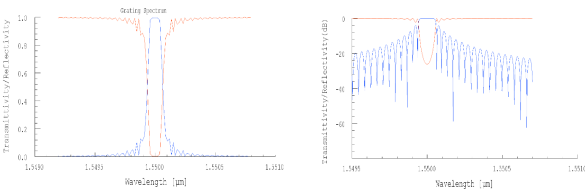

5(c) Reflectivity Spectrum at Grating Length of 20 mm 5(d) SLL Spectrum at Grating Length of 20 mm

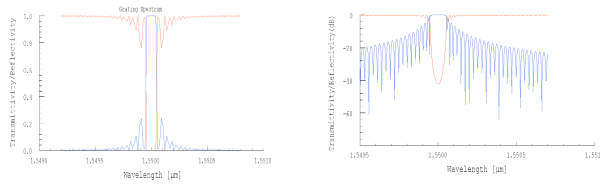

5(e) Reflectivity Spectrum at Grating Length of 30 mm 5(f) SLL Spectrum at Grating Length of 30 mm

Figure 5: Spectral Response of FBG at different Grating Length

It is observed that reflectivity increases with length. The effect of increased length on SLLs is shown in figure 5. The spectrum shows the increased side lobe levels at loner length. Table 2 illustrates the reflectivity and SLL values at different grating length. The reflectivity of the Fiber Bragg Grating increases with grating length, rising from approximately 88.5% at 10 mm to nearly 100% at 30 mm. This trend indicates that longer gratings enable stronger constructive interference of reflected light, producing a higher reflected peak. But increased length significantly affects SLL performance. Low SLLs of -24.54 dB are noticed at 10 mm.

Table 2: Reflectivity and SLL at different Grating Length

Grating Length L (mm)	Reflectivity	SLL	SLL (dB)
10	0.88415	0.05938	−24.54 dB

20	0.9974	0.25462	−11.89 dB
30	0.99993	0.32698	−9.71 dB

In medical sensing applications, higher reflectivity and low SLLs enhance the signal-to-noise ratio (SNR), allowing more precise detection of small wavelength shifts caused by physiological signals. Beyond 20 mm, the reflectivity curve begins to saturate, suggesting that further increasing the grating length provides minimal additional improvement in reflected intensity.

5.2 Effect of Modulation Index on Reflectivity and SLL.

The FBG spectral characteristics for different values are plotted as shown in figure 6. The change in modulation index changes both reflectivity and SLLs

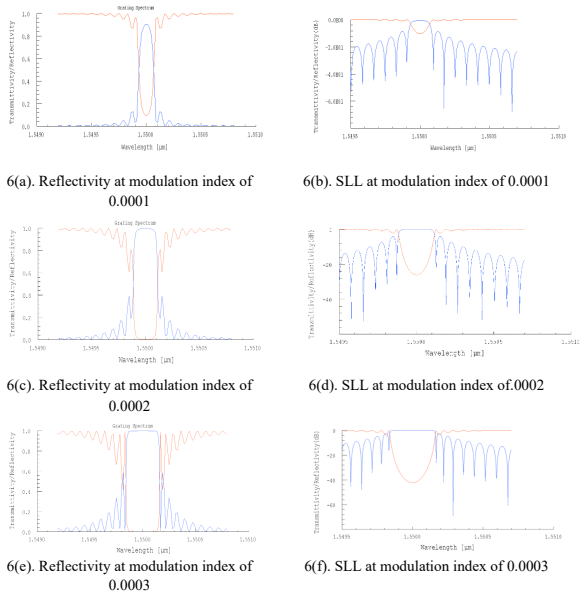

6(a). Reflectivity at modulation index of 0.0001

6(b). SLL at modulation index of 0.0001

6(c). Reflectivity at modulation index of 0.0002

6(d). SLL at modulation index of.0002

6(e). Reflectivity at modulation index of 0.0003

6(f). SLL at modulation index of 0.0003

Figure 6: Spectral Response of FBG at different Modulation Index

The reflectivity of the Fiber Bragg Grating increases sharply with the modulation index. For $n = 0.0001$, the reflectivity is around 90%, and it rises to nearly 100% for $n = 0.0003$. This rapid increase indicates that stronger refractive index modulation enhances the reflected peak intensity. However, beyond a certain point, the gain in reflectivity provides diminishing returns, as the SNR is already sufficiently high for accurate measurements.

Table 3: Reflectivity and SLL at different Modulation Index

Modulation Index	Reflectivity	SLL	SLL (dB)
0.001	0.904004	0.11461	−18.81 dB
0.002	0.997535	0.97378	−0.23 dB
0.003	0.99994	0.99965	−0.003 dB

The side lobe levels increase significantly with the modulation index, from approximately -18.81 dB for $n = 0.0001$to -0.003 dB for $n = 0.0003$. Higher SLL indicates stronger unwanted reflections adjacent to the main Bragg peak, which can interfere with accurate peak tracking. In the context of FBG-based medical sensors, excessive side lobes may reduce the wavelength resolution and compromise the precision of vital sign monitoring.

5.3 Analysis of Sensor Performance for different Apodization Techniques.

The apodization techniques are used to get desired performance of FBG sensor for medical applications. In this section the performance analysis is done for three different apodization profile to determine desired reflectivity and side lobe levels. The apodization is carried out with grating length of 10 mm, modulation index of 0.0003, Grating period of 0.5312 and core cladding dimension of 4.6 μm and 62.5 μm respectively.

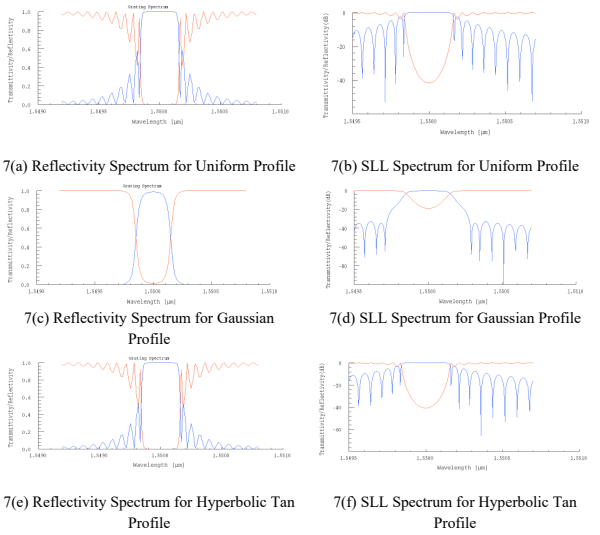

7(a) Reflectivity Spectrum for Uniform Profile

7(b) SLL Spectrum for Uniform Profile

7(c) Reflectivity Spectrum for Gaussian Profile

7(d) SLL Spectrum for Gaussian Profile

7(e) Reflectivity Spectrum for Hyperbolic Tan Profile

7(f) SLL Spectrum for Hyperbolic Tan Profile

Figure 7: Spectral Response of FBG for different Apodization Techniques

The reflectivity spectrum of a uniform FBG shows a sharp and well-defined peak at the Bragg wavelength. This indicates that the grating reflects a narrow band of wavelengths very efficiently, which is useful for precise sensing applications. The high peak reflectivity means that small wavelength shifts caused by strain or temperature changes can be easily detected. The SLL spectrum for the uniform profile typically shows noticeable side lobes adjacent to the main peak. These side lobes represent unwanted reflections at wavelengths near the Bragg wavelength and can introduce noise in the detection system. In practical terms, higher SLL can reduce the accuracy of wavelength shift detection, so uniform FBGs are often designed with optimization to minimize SLL.

Table 4: Performance Comparison of different Profiles

Apodization Profile	Reflectivity	SLL	SLL (dB)
Uniform	0.999931	0.130858	−17.67 dB
Gaussian	0.986991	0.000498	−66.06 dB
Hyperbolic Tan	0.999913	0.116631	−18.66 dB

The reflectivity spectrum of a Gaussian-apodized FBG is smoother compared to the uniform profile. While the main peak may be slightly lower than that of a uniform FBG, it still offers strong reflectivity of 98.69% at the Bragg wavelength. The Gaussian apodization reduces abrupt changes in the refractive index, which leads to the suppression of unwanted side lobes. The SLL of -66 dB shows significantly lower value than the uniform FBG, which improves the SNR and the accuracy of peak tracking. This makes Gaussian FBGs particularly suitable for high-precision medical sensing applications, where noise minimization is critical.

The reflectivity spectrum of a hyperbolic tangent profile FBG is also sharp and provides reflectivity of 99. 99% which is comparable with uniform profile. The SLL spectrum shows minimal side lobes of -18.66 dB, often lower than both uniform and Gaussian profiles. This reduction inside lobes is advantageous for detecting very small wavelength shifts with high fidelity, as the impact of nearby unwanted reflections is minimized.

The comparison of spectral response of these profiles shows that gaussian apodization can provide desired reflectivity and much improved SLLs. They offer high SNR and hence the high sensitivity in noisy environments. Hence, gaussian apodised FBG sensor is more suitable in clinically noisy environment for precise measurement of healthcare parameters.

6. Conclusion

The Performance of FBG sensor for Grating length and modulation index is investigated. Increasing grating length and modulation index improves the reflectivity but SLL also increases. This is undesirable in high precision sensing applications. Uniform grating offers structural simplicity and high reflectivity. Due to its high side lobe levels its sensitivity is low. Uniform grating profile FBG can provide high reflectivity and moderate SLL suppression. The better sidelobe level suppression is done by using apodization. In medical sensing application reflectivity, more than 90 % and side leobe level less than -20 dB are desirable. The comparative analysis shows that Gaussian profile gives excellent side lobe suppression over uniform and hyperbolic tan profile. Based on the findings of this research work, we propose the gaussian profile FBG sensor with grating length of 10 mm and modulation index of 0.0003. The proposed gaussian FBG sensor gives high reflectivity of 98.69% and excellent side lobe level suppression of -66 dB. The proposed FBG sensor is more promising in a medical application where high precision is required for accurate diagnosis.

REFERENCES

1. Daniel Krizan et al., “Embedding FBG sensors for monitoring vital signs of the human body: Recent progress over the past decade,” APL Photonics, 2024.
2. E. Mbunge et al., “Sensors and healthcare 5.0: Transformative shift in virtual care through Emerging Digital health Technologies,” Global Health Journal, vol. 5, Issue 4, Pages 169-177, 2021.
3. Alhussein et al., “Fiber Bragg Grating Sensors: Design, Applications, and Comparison with Other Sensing Technologies,” Sensors 2025.
4. Braunfelds, et al., “Designing of Fiber Bragg Gratings for Long-Distance Optical Fiber Sensing Networks,” Modelling and Simulation in Engineering,”. pp. 1-14. 2022.
5. Chaluvadi et al., “Recent advancements in fiber Bragg gratings-based temperature and strain measurement,” Results in Optics, vol. 5, 2021.
6. Khorasani Sina & Rashidian Bizhan, “Modified transfer matrix method for conducting interfaces,” Journal of Optics A: Pure and Applied Optics, 2021.
7. Praena & Carballar,” Integrated Bragg Grating Spectra,” Photonics. 2025.
8. Onoufriou et al.,”Fibre Bragg Gratings,” Springer series in optical sciences, 2006
9. Fahd et al., “Apodization Optimization of FBG Strain Sensor for Quasi-Distributed Sensing Measurement Applications,” Active and Passive Electronic Components, 2016.
10. Saktioto et al., “Integration of chirping and apodization of Topas materials for improving the performance of fiber Bragg grating sensors,” Journal of Physics: Conference Series,2021.
11. Tahhan et al., ‘Characteristics of Chirped Fiber Bragg Grating Dispersion Compensator Utilizing Two Apodization Profiles,” Journal of Communications. vol. pp. 13. 108-113, 2018.
12. Elleithy et al., “Investigating the Performance of Apodized Fiber Bragg Gratings for Sensing Applications,” Conference of the American Society for Engineering Education, 2014.
13. Onoufriou et al.,”Fiber Bragg Gratings: Fundamentals and Applications in Telecommunications and Sensing,” Physics Today, 2000.
14. P. V. Raja Shekar, “Optimal parameters for fiber Bragg gratings for sensing applications: a spectral study,” SN Applied Science, 2021.